JOURNAL OF SOLID STATE CHEMISTRY 115, 214–224 (1995)

Synthesis and Characterization of $KAlSiO_4$ Polymorphs on the SiO_2-$KAlO_2$ Join

II. The End Member of ANA Type of Zeolite Framework

R. Dimitrijevic* and V. Dondur†

*Faculty of Mining and Geology, Department of Mineralogy and Crystallography, Belgrade University, Djušina 7, 11000 Belgrade, Yugoslavia; and †Institute of Physical Chemistry, Faculty of Sciences and Mathematics, Belgrade University, P.O. Box 550, Belgrade, Yugoslavia

Received July 15, 1993; in revised form April 18, 1994; accepted July 13, 1994

High-temperature phase transformations of K-LTA zeolite were investigated in the temperature range 800–1500°C. The nanostructured $KAlSiO_4$ precursor was prepared at 850°C and after annealing at 1000°C, the first polymorph of $KAlSiO_4$, synthetic kaliophilite was formed. With increasing temperature, the following polymorphs were synthesized: kalsilite (1100°C), low $KAlSiO_4$-O_1 (1200°C), $KAlSiO_4$-ANA (1300°C), and high $KAlSiO_4$-O_2 at (1430°C). Synthetic kaliophilite and $KAlSiO_4$-ANA phases are the new polymorphs in the system studied. Consequently, the $KAlSiO_4$-ANA phase is the ANA-type end member of the zeolite framework having the ratio Si/Al = 1. From XRD powder patterns a distorted leucite unit cell for a $KAlSiO_4$-ANA phase was calculated: a_0 = 13.638(6) Å, b_0 = 13.811(8) Å, c = 13.817(9) Å, α_0 = 99.98(4)°, β_0 = 102.28(4)°, and γ_0 = 62.80(4)°. ^{29}Si MAS NMR chemical shifts at −89.08 and −98.01 ppm suggest that the $KAlSiO_4$-ANA phase has an ordered framework cation topology.

INTRODUCTION

Different aluminosilicate minerals from the system (1) K_2O–Al_2O_3–SiO_2 (KALSI) (Fig. 1a), were the object of much interest as a key for the elucidation of the crystallization history of alkaline rocks. Their common crystallochemical feature is a framework topology consisting of corner-linked (Al, Si)O_4 tetrahedra containing interstices filled with K^+ cations. Another characteristic of the minerals from the KALSI system is the isomorphous replacement of Si^{4+} by Al^{3+} cations in tetrahedral positions. The framework topology of potassium feldspars (2) is characterized by single four- and eight-membered tetrahedrally connected rings and a Si/Al = 3 ratio. The crystal structures of leucite minerals (3–5) (ratio Si/Al = 2) consist of single four-, six-, and eight-membered connected tetrahedra rings as in analcime (6).

In the region of Si/Al = 1 composition of the KALSI phase diagram (7) (Fig. 1b), several natural and synthetic polymorphs are known (7–9). Their framework topologies are based on stuffed derivatives (10) of tridymite (11). The kalsilite structure (12–14) consisting of mutually connected single six-membered tetrahedra rings is a representative. The phase relationships between kalsilite and thermally induced (15–18) $KAlSiO_4$ polymorphs ($KAlSiO_4$-O_1, $KAlSiO_4$-O_2, synthetic kaliophilite (19), and natural kaliophilite (20)) were treated by several authors (7–9, 11). The structural details of these $KAlSiO_4$ phases and of kalsilite (18) at 950°C are, however, unknown.

Due to their open structure and the possibility of modifications, zeolites are potential precursors in the synthesis of new materials by thermal transformations (21–27). Some rock-forming minerals such as nepheline (25) and anorthite (27) were synthesized by this procedure, also.

In a previous paper (22) we have presented the results obtained on the synthesis of $CsAlSiO_4$-ANA (low and high) phases upon high-temperature treatment of the Cs-LTA framework. The results published for the Cs-LTA precursor as well as those presented earlier for alkaline (21, 25, 26) cations show that an ordered LTA zeolite framework is an excellent medium for the investigation of phase relationships in the M_2O–Al_2O_3–SiO_2 (M, alkaline cation) phase systems, particularly those on the $MAlO_2$–SiO_2 join. In this paper we report the results obtained on thermal treatment of the K-LTA precursor in a three-component KALSI phase system.

EXPERIMENTAL

Zeolite LTA (6) manufactured by Union Carbide Co. was used as the starting material. A fully exchanged K^+ form of LTA zeolite was prepared from KCl solution in the same manner as that reported in the papers on the crystal structure of K-LTA zeolite (28, 29). Potassium-

0022-4596/95 $6.00

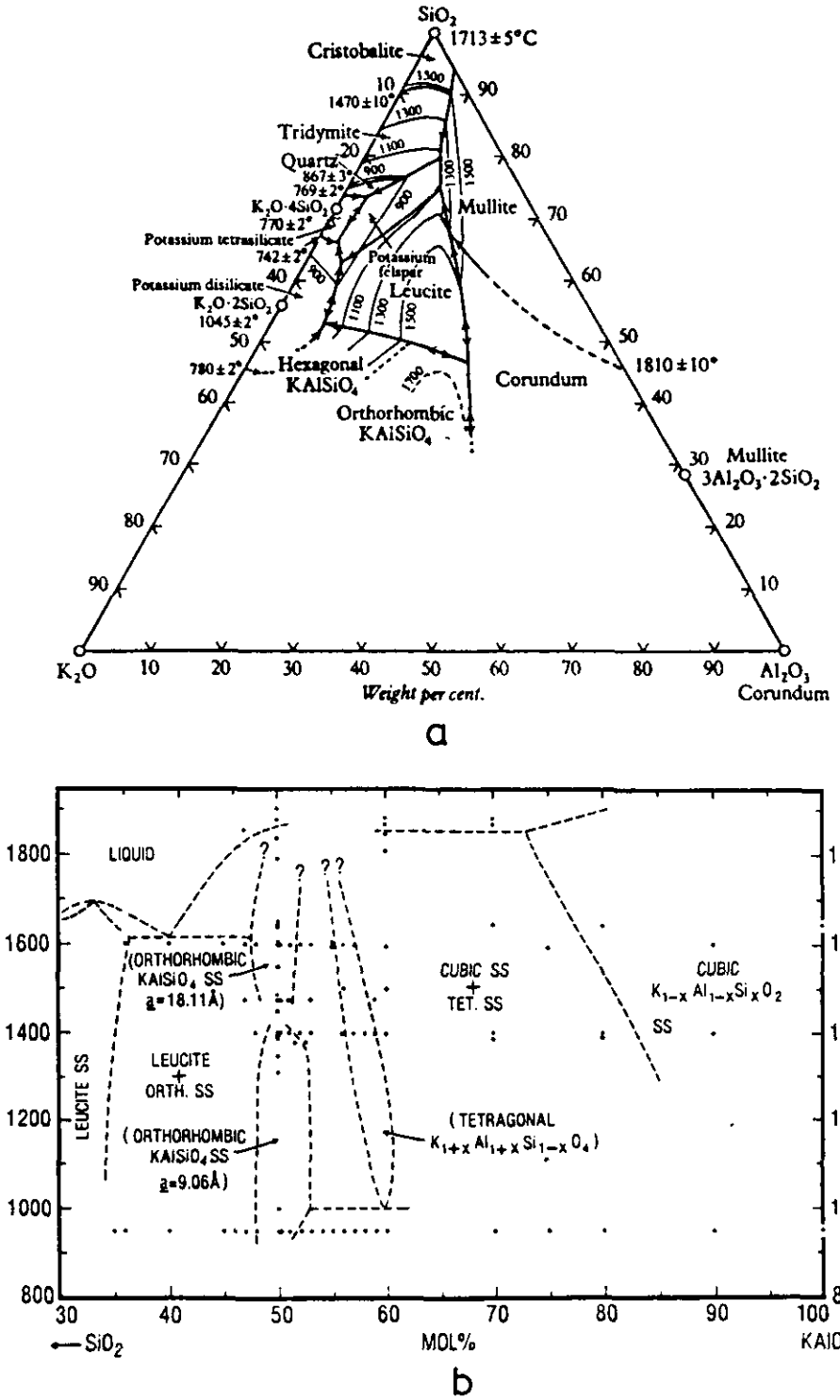

FIG. 1. KALSI phase system: (a) ternary system K_2O–Al_2O_3–SiO_2 after Schairer and Bowen (1) and (b) part of the SiO_2–$KAlO_2$ system following Cook *et al.* (7).

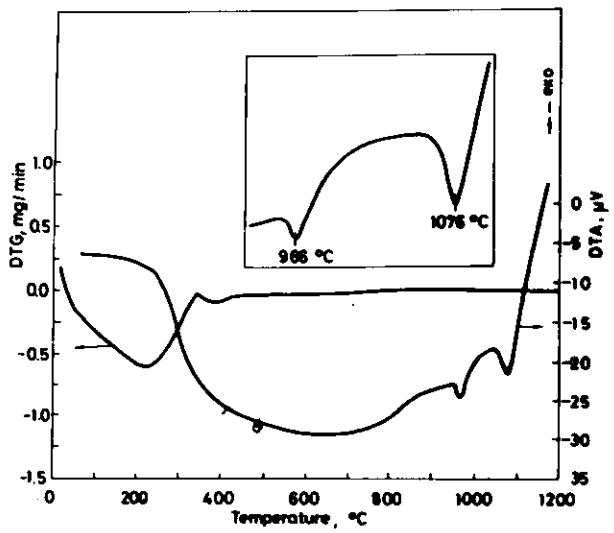

FIG. 2. DTA and DTG curves of K^+-exchanged LTA zeolite.

exchanged zeolites, with SOD (sodalite), GIS (Na–P), and FAU (X and Y) framework topologies used for the comparison of the results, were synthesized in our laboratory.

The chemical compositions of the samples were analyzed using a Perkin–Elmer 380 atomic absorption spectrophotometer.

The thermal behavior of K-LTA, K-SOD, K-GIS, and K-FAU zeolite frameworks before they collapsed into amorphous precursors was investigated using a Netzsch Model STA-409 EP simultaneous thermal analyzer, equipped with high-temperature DTA (1200°C) and DSC cells, at heating rates of 10 and 5°C per minute. Before the X-ray diffraction measurements were performed, samples were heated in the Netzsch 421 type furnace at different temperatures in the range from 30 min to 3 hr to a constant temperature with an error of ±5°C. All X-ray diffraction experiments were done after cooling to room temperature.

The X-Ray powder diffraction (XRD) patterns were obtained on a Philips PW-1710 automated diffractometer, using a Cu tube operated at 40 kV and 35 mA. The instrument was equipped with a diffracted beam curved graphite monochromator and a Xe-filled proportional counter. Diffraction data were collected in the range 2Θ, 4° to 90°, counting for 2.5 and 8.05 sec at 0.02 steps. A fixed 1° divergence and 0.1° receiving slits were used. Silicon powder was used as a standard for the calibration of the diffractometer. The trial and error indexing programs Treor-4 (30) and Visser (31) and a program for the refinement of cell dimensions Lsucripc (32) were used.

^{29}Si MAS NMR spectra were measured at 79.5 MHz with a Bruker MSL-400 multinuclear spectrometer. An Andrew–Beams probehead was used with rotors spinning at 5 KHz with air as the driving gas. Radio frequency pulses equivalent to a 54° pulse angle were applied with 12 sec recycle delay. ^{29}Si chemical shifts are quoted in ppm from external tetramehtylsilane (TMS). ^{27}Al chemical shifts are reported relative to an external 1 *M* $AlCl_3$ solution.

Infrared absorption spectra were recorded on a Perkin–Elmer Model 983 grating spectrophotometer, using a KBr pellet technique.

RESULTS

The results of chemical analyses show that complete $K^+ \rightarrow Na^+$ exchange on Na-LTA zeolite was achieved. The cell dimensions of K-LTA zeolite (a_0 = 12.296(1) Å) were found to be 3σ of 12.301(2) Å, as given by Leung *et al.* (28). Thermal effects on DTA and TG curves in the temperature range from room temperature to 1200°C (Fig. 2) can be ascribed to the dehydration of (216 and 563°C) K-LTA zeolite and consecutive phase transitions (966 and 1076°C). After dehydration at 563°C, K-LTA structure collapses into an amorphous K_2O–Al_2O_3–SiO_2 precursor which was used as the starting material in our further investigations. High-temperature investigations of this precursor were started at 900°C and the recrystallization was followed up to 1500°C.

The amorphous K_2O–Al_2O_3–SiO_2 began to recrystallize at 950°C and at 1000°C, after 1 hr annealing, a phase similar to synthetic kaliophilite (8, 19) was formed. The crystallization of this phase was accompanied by the appearance of an exothermal peak at 966°C on the DTA curve (Fig. 2). The XRD pattern of a $KAlSiO_4$ phase similar to synthetic kaliophilite is shown in Fig. 3a; unit cell dimensions are presented in the Table 1, while MAS NMR and IR spectral data are given in Tables 2 and 3 and Figs. 5a and 6a.

On further calcination, the synthetic kaliophilite-like phase starts to transform into the kalsilite. An exothermal peak at 1076°C (Fig. 2) belongs to this transformation.

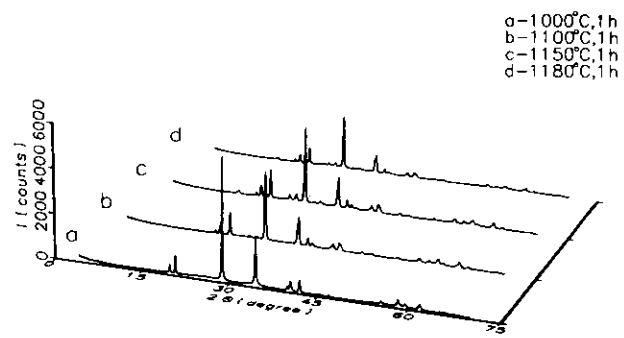

FIG. 3. Polymorphous transformation of $KAlSiO_4$ in the temperature range 1000–1200°C. XRD powder patterns of: (a) synthetic kaliophilite, (b) kalsilite, and (c) and (d) solid–solid topotactic transition of kalsilite to $KAlSiO_4$-O_1 phase. Scan 2.50 sec, step 0.02°.

TABLE 1
Unit Cell Dimensions of the Investigated $KAlSiO_4$ Polymorphs

Sample	a_0 (Å)	b_0 (Å)	c_0 (Å)	α_0 (°)	β_0 (°)	γ_0 (°)	v_0 (Å)^3
Synt. kaliophilite K-LTA at 1000°C, 1 hr	5.197(1)	5.197(1)	8.583(5)	90.00	90.00	120.00	200.8(2)
Synt. kalsilite K-LTA at 1100°C, 1 hr	5.160(1)	5.160(1)	8.632(6)	90.00	90.00	120.00	199.1(4)
$KAlSiO_4$-O_1 (low) K-LTA at 1200°C, 3 hr	13.638(4)	13.782(6)	13.743(5)	100.11(2)	102.42(3)	62.84(2)	2236(2)
$KAlSiO_4$-ANA K-LTA at 1300°C, 3 hr	13.638(6)	13.811(8)	13.817(9)	99.98(4)	102.28(4)	62.80(4)	2253(3)
$KAlSiO_4$-O_2 (high) K-LTA at 1430°C, 1/2 hr	13.667(5)	13.809(7)	13.851(7)	100.12(3)	102.42(3)	62.78(2)	2261(2)

After heating for 1 hr pure kalsilite is formed at 1100°C. Chemical analysis of this phase gave the composition SiO_2 = 38.17%, Al_2O_3 = 31.95%, K_2O = 29.70%, Na_2O = 0.09%, Σ = 99.91% corresponding to the crystallochemical formula.

$$(K_{0.998}Na_{0.004})_{1.002}(Al_{0.991}Si_{1.005})_{1.996}O_{4.000}.$$

These results suggest synthesis of pure kalsilite and the complete exchange of K^+ for Na^+ cations on the LTA framework, also. The results of XRD investigations are presented in Fig. 3b and Table 1, while spectral data are given in Tables 2 and 3 and Figs. 5b and 6b.

The kalsilite phase is unstable upon further temperature increase and gives rise to XRD superstructure lines (Figs. 3c and d) which could not be indexed on a hexagonal (12) unit cell. This instability of the kalsilite phase in the range 1100 to 1200°C is apparent from the DTA curve in Fig. 2. The polymorphic transformation of the kalsilite phase was completed at 1200°C after 3 hr heating where the $KAlSiO_4$ phase resembling that of the $KAlSiO_4$-O_1 phase (7–9) (JCPDS file card 33-988) was formed. Diffraction data for the $KAlSiO_4$ phase at 1200°C are listed in Tables 1 and 4. The XRD pattern is shown in Fig. 4a and the spectral data are presented in Figs. 5c and 6c and Tables 2 and 3.

TABLE 2
Chemical Shifts for ^{29}Si and ^{27}Al MAS NMR of $KAlSiO_4$ Polymorphs

Sample	^{29}Si Chemical shifts (ppm)	^{27}Al Chemical shifts (ppm)
Synt. kaliophilite K-LTA at 1000°C, 1 hr	−88.15	64.98
Synt. kalsilite K-LTA at 1100°C, 1 hr	−89.63	66.27
$KAlSiO_4$-O_1 (low) K-LTA at 1200°C, 3 hr	−89.17, −98.02	65.73
$KAlSiO_4$-ANA, K-LTA at 1300°C, 3 hr	−89.08, −98.01	65.60
$KAlSiO_4$-O_2 (high) K-LTA at 1430°C, 1/2 hr	−89.09, −98.07	65.71

Continued thermal treatment in the temperature range 1200 to 1300°C of $KAlSiO_4$-O_1 caused drastic changes in the intensity of reflections which were most intense at 1300°C. The $KAlSiO_4$ phase formed at 1300°C had an XRD pattern very similar to that of leucite (JCPDS file card 38-1423) but with many superstructure lines. The indexed powder pattern of the latter phase is presented in Table 4. The unit cell dimensions are given in Table 1. MAS NMR and IR spectral data for leucite similar $KAlSiO_4$ polymorph are given in Tables 2 and 3 and Figs. 5d and 6d.

Polymorphic transitions are not completed at 1300°C and prolonged heating up to 1450°C caused a novel $KAlSiO_4$ phase transition. The XRD patterns obtained in the range 1300 to 1400°C showed a tendency of decreasing peaks intensities in the 2Θ angle range of 20°–30° (Fig. 4c), in contrast to increasing intensities of the same peaks between 1200 and 1300°C. The results of the $KAlSiO_4$ synthesis performed at 1430°C after 30 min calcination resulted in a powder pattern shown in Fig. 4d and Table 4. This pattern could be identified as $KAlSiO_4$-O_2 (high polymorph, JCPDS file card 33-989). The unit cell dimensions for this phase are presented in Table 1, while spectral characteristics are given in Tables 2 and 3, and Figs. 5e and 6e.

Experimental investigations ended at 1500°C after 1 hr annealing, where the crystal structure of the $KAlSiO_4$-O_2 phase collapsed into amorphous K_2O–Al_2O_3–SiO_2 glass and traces of corundum.

DISCUSSION

Formation of K_2O–Al_2O_3–SiO_2 Precursor

The structure of K-LTA zeolite in a hydrated (28) as well as a dehydrated (28, 29) state has been recently

TABLE 3
Infrared Absorption Bands of the Investigated $KAlSiO_4$ Polymorphs

Sample	ν_{as} T–O–T (cm^{-1})					ν_s T–O–T (cm^{-1})								δ O–T–O (cm^{-1})					
Synt. kaliophilite K-LTA at 1000°C, 1 hr	1100(sh)		1035	980	940			690		645			595	550		475		450	425
Synt. kalsilite K-LTA at 1100°C, 1 hr			1030	980	955			685		650(sh)		605	595	550		470			
$KAlSiO_4$-O_1 (low) K-LTA at 1200°C, 3 hr	1100	1070	1040	990	940	880(sh)		765	700	665		630(sh)	605	540	520		465	440	425
$KAlSiO_4$-ANA K-LTA at 1300°C, 3 hr	1100		1040	990	950	875	820(sh)	765	700	670(sh)		635	605	575(sh)	540		475(sh)	460	435
$KAlSiO_4$-O_2 (high) K-LTA at 1430°C, 1/2 hr	1100	1070	1040	1000	960	880(sh)	820(sh)	765	695	670(sh)		625(sh)	605	540	520(sh)		645	440	430

solved. Most of the 12 K^+ cations per unit cell of the dehydrated phase were located in the vicinity of S6R tetrahedra rings. A full ordering of Si^{4+} and Al^{3+} cations in the LTA framework was confirmed (29). From the curves in Fig. 2, obtained by thermal investigations, it can be seen that the starting K-LTA zeolite in the course of heating from room temperature to 400°C passes through a dehydration process which is accompanied by consecutive phase transitions (33) before the framework collapses between 700–800°C.

The amorphous precursor starts to recrystallize at 900°C (exothermal maxima at 966°C), and the crystallization of that phase is completed at 1000°C after 1 hr calcination. The recrystallization followed in a narrow temperature range suggests a nanocrystalline character for the K_2O–Al_2O_3–SiO_2 precursor.

Synthetic Kaliophilite → Kalsilite Transition

The XRD pattern of the $KAlSiO_4$ phase formed at 1000°C (Fig. 3a) can only be compared with synthetic kaliophilite published by Smith and Tuttle (8) and Rigby and Richardson (19). They reported powder patterns of kalsilite with very weak diffraction peaks 111, 113, and 115 in the unannealed material, but when heated to near 400°C, the relative intensity increases irreversibly. Similar effects on these reflections were noted by Abbott (11), Dollase and Freeborn (13), and Capobianco and Carpenter (17) in the course of a single crystal investigation of kalsilite. In our experiment we also have observed the reversibility of these diffraction effects. The powder pattern of the $KAlSiO_4$ phase obtained at 1000°C is characterized by the disappearance of some kalsilite reflections. Reflections of the forms $(h0l)$ and (hhl) with $l = 2n + 1$ are systematically absent in the observed powder pattern (Fig. 3a). This phase is very close to being dimensionally hexagonal as kalsilite observed at 1100°C (Fig. 3b and Table 1), but powder data for synthetic kaliophilite (34) could be indexed in orthorhombic symmetry with $a_{orth} = 2.5974(4)$ Å, $b_{orth} = 4.502(2)$ Å, $c_{orth} = 4.292(2)$ Å, and $V_{orth} = 50.19(5)$ Å^3. This unit cell, in terms of the traditional hexagonal cell, is given by $a_{orth} = a_{hex}/2$; $b_{orth} = a_{hex}(\sqrt{3}/2)$; $c_{orth} = c_{hex}/2$; $V_{orth} = V_{hex}/4$. Although we cannot say with absolute certainty (missing of single crystal measurements) that our synthetic kaliophilite is the new phase in the KALSI system, we believe this to be the case. Accordingly, we have decided to keep the term fsynthetic kaliophilite following the nomenclature used by Abbott (11) and Capobianco and Carpenter (17). Prolonged heating of synthetic kaliophilite at 1100°C for 1 hr proceeds in a polymorphous transition to common hexagonal kalsilite (Fig. 3b, Table 1).

MAS NMR data presented in Table 2 and Figs. 5a and 5b for synthetic kaliophilite and the kalsilite phases suggest completely ordered (Al, Si)O_4 frameworks. Unfortunately, the ^{29}Si and ^{27}Al MAS NMR spectra for synthetic kaliophilite and pure hexagonal kalsilite are

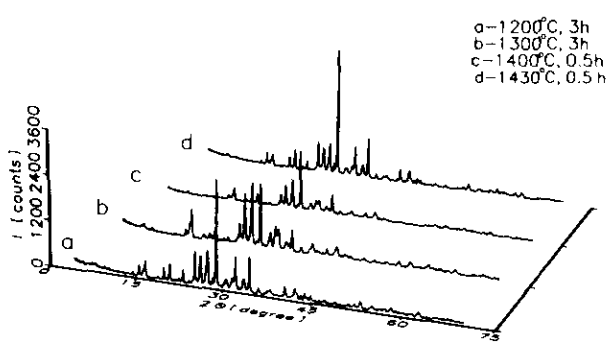

FIG. 4. Polymorphous transformation of $KAlSiO_4$ in the temperature range 1200–1500°C. XRD powder patterns of (a) $KAlSiO_4$-O_1 phase, (b) $KAlSiO_4$-ANA phase, (c) intermediate $KAlSiO_4$ phase, and (d) $KAlSiO_4$-O_2 phase. Scan 2.50 sec, step 0.02°.

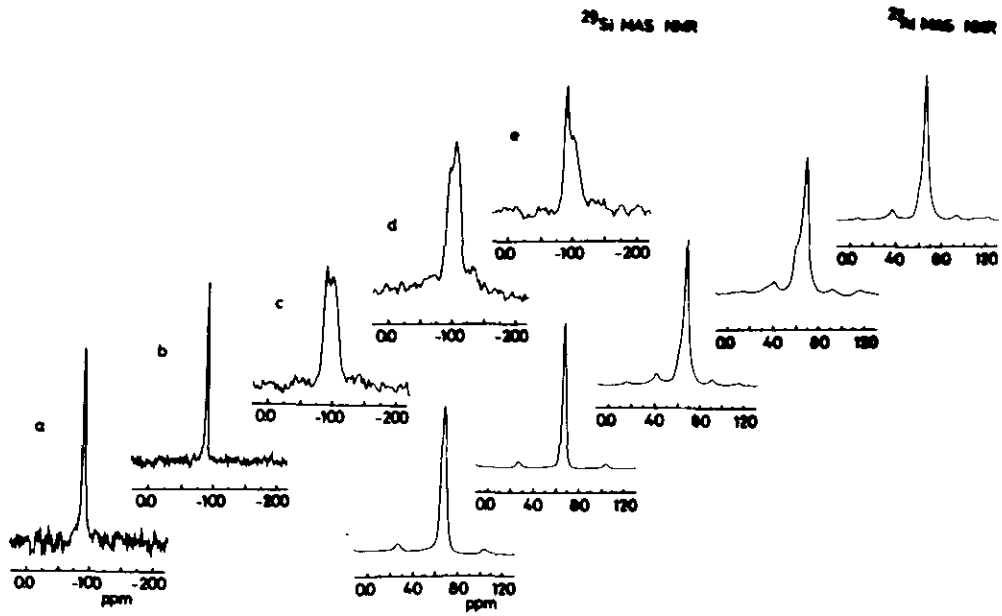

FIG. 5. ^{29}Si and ^{27}Al MAS NMR spectra of $KAlSiO_4$ polymorphs: (a) synthetic kaliophilite, (b) kalsilite, (c) $KAlSiO_4$-O_1 phase, (d) $KAlSiO_4$-ANA phase, and (e) $KAlSiO_4$-O_2 phase.

not available. Recently reported results by Stebbins (35) *et al.* and Hovis (36) *et al.* which clearly show the existence of naturally occurring disordered kalsilite phase point to the existence of siliceous kalsilite in alkaline rocks.

From IR spectral data (Table 3 and Fig. 6a and 6b), it is obvious that both synthetic kaliophilite and kalsilite phases exhibit the same spectra, with minor discrepancies arising near 460 cm^{-1}. In the case of the synthetic kaliophilite, the latter peak is resolved in two bands at 475 and 450 cm^{-1}. It is worth noting that both samples display absorptions at 640 cm^{-1}, 595 cm^{-1}, and 550 cm^{-1}, respectively, which are not found in the spectrum of kalsilite synthesized by Henderson and Taylor (37).

In view of our results obtained for synthetic kaliophilite and kalsilite phases, and taking into account their similarities, it is evident that the same aluminosilicate framework is involved, namely, the same topological ordering of (Al, Si)O_4 tetrahedra. According to the topological systematization of aluminosilicate structures (38) and on the basis of linking of 6^3 tetrahedral sequences it is clear that synthetic kaliophilite formed at 1000°C belongs to the second type. It is characterized by CCCCCC orientation and 6^6 ordering of tetrahedra as in the case of kalsilite (39). On the basis of the presented results and of considerations relating to synthetic kaliophilite–kalsilite polymorphous transition in the temperature range 1000–1100°C, it may be concluded that this transition is displacive, caused primarily by the mobility of K^+ cations on the ordered (Si, Al)O_4 framework. The crystal structures of synthetic kaliophilite and kalsilite are under investigation and will be reported (34) separately.

The Topotactic Transformation Kalsilite → $KAlSiO_4$-O_1

Continued heating of the kalsilite sample gives rise to the appearance of numerous superstructure reflections in the XRD powder pattern. The kalsilite samples annealed at 1150 and 1180°C (Figs. 3c and 3d) are very similar to that of natural kaliophilite (JCPDS card 11-313), and superstructure reflections could be assigned to the kalsilite unit cell after multiplying a_0 by $3\sqrt{3}$ (8, 20). With progressive heating these reflections increased their intensities and at 1200°C, the XRD pattern proceed in $KAlSiO_4$-O_1 phase. It is obvious that during heating in the range 1100 to 1200°C, kalsilite undergoes a slow reconstructive transformation to a high temperature $KAlSiO_4$-O_1 polymorph. This is consistent with the results published by Capobianco and Carpenter (17), Stebbins *et al.* (35) and Tuttle and Smith (40). We believe that naturally occuring kaliophilite (20, 41) is probably an intermediate phase of the thermally induced polymorphic transformation of kalsilite into the $KAlSiO_4$-O_1 phase.

The differences between kalsilite and the $KAlSiO_4$-O_1 phase formed at 1200°C, could be the best perceived by comparing their XRD patterns (Figs. 3b and 4a) and ^{29}Si and ^{27}Al MAS NMR spectra (Figs. 5a and 5c). From infrared absorption spectra (Figs. 6b and 6c, and Table 4) it can be seen that the most pronounced differences between kalsilite and $KAlSiO_4$-O_1 phase appear in the absorp-

TABLE 4
XRD Powder Data of the Investigated $KAlSiO_4$ Polymorphs

			$KAlSiO_4$-O_1 phase at 1200°C			$KAlSiO_4$-ANA phase at 1300°C			$KAlSiO_4$-O_2 phase at 1430°C		
h	k	l	I/I_o (%)	d_{obs} (Å)	d_{calc} (Å)	I/I_o (%)	d_{obs} (Å)	d_{calc} (Å)	I/I_o (%)	d_{obs} (Å)	d_{calc} (Å)
0	1	0	3.11	12.2179	12.2130						
1	1	0	3.91 R	11.3268	11.3868	6.81	11.3341	11.4089	2.64 R	11.3051	11.4142
0	−1	1	2.07	9.4332	9.4467	4.09	9.4483	9.4733	1.05	9.4634	9.4859
0	1	1	1.03	8.6677	8.6422						
−1	1	0	0.75 R	7.1008	7.1417						
−1	−2	1	0.81	6.5298	6.5417	2.56	6.5370	6.5548	0.45	6.5732	6.5606
1	−1	1	2.90	6.2021	6.1983	2.77	6.2108	6.2082	2.64	6.2173	6.2148
0	−2	1	9.79	5.7665	5.7518	10.75	5.7703	5.7626	9.60	5.7684	5.7652
0	1	2	2.50	5.6586	5.6559	5.91	5.6693	5.6876			
1	2	1						5.6517	1.45	5.6586	5.6470
1	0	2				17.44	5.5219	5.5172	4.44	5.5151	5.5237
2	1	1	6.46	5.4880	5.4918						
0	2	1	14.48	5.3846	5.3765	46.50	5.3837	5.3945	9.18	5.3885	5.3910
2	2	1	0.95	4.8530	4.8526				0.65	4.8715	4.8693
−2	0	2			4.8501						4.8700
0	−2	2	2.41	4.7237	4.7233	7.69	4.7337	4.7366	1.30	4.7349	4.7429
−2	1	1	9.87	4.5063	4.5055	10.75	4.5097	4.5073	9.46	4.5142	4.5134
−1	−3	1									
−2	−3	1				7.07	4.4383	4.4381	1.64	4.4438	4.4410
1	−2	1						4.4338			4.4365
−3	−2	1	2.22	4.4121	4.4117						
−1	2	1			4.4056						
2	−1	1	16.04	4.2724	4.2732	15.97	4.2826	4.2771	14.72	4.2877	4.2822
2	1	2						4.2873			4,2899
3	0	0				3.10	3.9917	3.9961	2.53	3.9971	4.0032
−2	−2	3	2.98	3.9855	3.9805						
−1	1	3	10.75 R	3.8579	3.8502	8.62	3.8675	3.8677	7.52	3.8728	3.8725
3	2	1			3.8556			3.8650			3.8674
−3	0	2	1.93	3.6928	3.6899				1.93	3.6928	3.6899
0	−3	2				8.62 R	3.6180	3.6313			
3	3	1									
−2	2	0	31.44 R	3.5436	3.5708	31.68 R	3.5617	3.5725	25.00 R	3.5555	3.5751
−3	−2	3	R		3.5304						
1	3	2				13.47	3.5092	3.5035			
−3	−1	3						3.5141			
−1	3	0	26.46	3.4256	3.4272	77.60	3.4347	3.4317	18.57	3.4340	3.4316
−2	−4	1						3.4392			3.4395
−4	−2	1	25.57	3.4018	3.4050				17.97	3.4108	3.4125
−4	−1	1							8.77 R	3.3111	3.3210
3	2	2									3.3103
0	−1	4	15.05	3.2979	3.3000						
−1	3	1			3.2954						
−1	−2	4							21.77	3.2700	3.2671
−3	−4	1	33.58	3.2612	3.2622	98.05	3.2676	3.2680			3.2699
4	1	0			3.2582						
−1	−4	2	8.29	3.1598	3.1586	10.12	3.1669	3.1652	7.46	3.1691	3.1669
4	3	0			3.1582						
−3	1	2			3.1595						
2	−2	2	100.00	3.0985	3.0992	100.00	3.1043	3.1041	100.00	3.1080	3.1074
1	0	4			3.0990						
0	−4	1				4.85	3.0371	3.0412			
4	1	1						3.0371			
−2	−4	3	2.81	2.9718	2.9718						
1	3	3	7.44	2.9450	2.9440	11.96	2.9560	2.9594	5.15	2.9550	2.9581

TABLE 4—*Continued*

			$KAlSiO_4$-O_1 phase at 1200°C			$KAlSiO_4$-ANA phase at 1300°C			$KAlSiO_4$-O_2 phase at 1430°C		
h	*k*	*l*	I/I_o (%)	d_{obs} (Å)	d_{calc} (Å)	I/I_o (%)	d_{obs} (Å)	d_{calc} (Å)	I/I_o (%)	d_{obs} (Å)	d_{calc} (Å)
−1	−3	4				23.16	2.9201	2.9195	5.47	2.9243	2.9255
−4	−3	3	8.00	2.90146	2.9145			2.9175			2.9257
−2	2	3	10.59	2.8400	2.8422	32.23	2.8471	2.8498			
−2	3	0			2.8416				7.27	2.8440	2.8450
0	2	4						2.8438			2.8452
−2	1	4									2.8448
−2	3	1	29.37	2.7861	2.7856	31.31	2.7891	2.7888	23.41 R	2.7921	2.7900
−3	0	4						2.7911			2.7980
0	4	2	7.72	2.6853	2.6882						
−4	0	3			2.6863	13.35	2.6888	2.6882			
−1	3	3						2.6865	8.10	2.6880	2.6868
0	0	5						2.6900			
−5	−2	2	12.11	2.6709	2.6724						
−3	4	2									
−3	−5	2							8.70	2.6709	2.6707
1	−4	1	10.43	2.6613	2.6616				R		2.6655
5	2	0			2.6610				R		2.6664
3	4	2			2.6619						2.6713
4	3	2				8.91	2.6396	2.6388			
0	−4	3						2.6367			
2	−3	2				30.22	2.6060	2.6086	32.78	2.6079	2.6108
−4	−1	4	34.36 R	2.5991	2.5942			2.5983			2.6060
−2	2	4	4.80	2.4904	2.4900				3.23	2.4994	2.5014
1	1	5									2.4975
0	3	4				7.96	2.4901	2.4900			
			48 NI lines up to 70° 2θ			35 NI lines up to 70° 2θ			51 NI lines up to 70° 2θ		

Note. NI, Nonindexed lines; R, rejected line.

tion bands within 550–850 cm^{-1} (ν_s T–O–T symmetrical stretching mode) and 400–550 cm^{-1} (δ O–T–O bending mode) regions. These spectral data suggest different framework topologies between the structure of kalsilite and $KAlSiO_4$-O_1 phase.

$KAlSiO_4$-O_1 → $KAlSiO_4$-ANA → $KAlSiO_4$-O_2 Transition

In the literature the $KAlSiO_4$-O_1 phase formed at 1200°C after 3 hr annealing could be found (7) under the name orthorhombic $KAlSiO_4$, also. Although this phase was discovered nearly 100 years ago (8) (Ref: A. Duboin (1892), N. L. Bowen (1917)), its crystal structure is still unknown. The powder patterns reported (7, 8) for the low-temperature $KAlSiO_4$-O_1 phases differ one from another in the number of superstructure lines observed, which can be due to different synthesis routes and appropriate structural states. Based on single crystal measurements, several orthorhombic (7–9, 11) and monoclinic (42) space groups for the $KAlSiO_4$-O_1 phase were considered and reported. Numerous efforts to index the powder pattern of the $KAlSiO_4$-O_1 phase synthesized in our experiment, based on higher (7–9, 42) symmetry, were unsuccessful. Indexing on the basis of a triclinic unit cell, however, is reported although monoclinic symmetry cannot be excluded.

Further heating of the $KAlSiO_4$-O_1 phase produces new changes in the XRD powder patterns (Fig. 4). The phase formed at 1300°C, which will be discussed below, on further annealing at 1430°C, is again polymorphously transformed into the $KAlSiO_4$-O_1 pattern (high $KAlSiO_4$-O_2 phase, JCPDS card 33-988). The XRD powder patterns of the $KAlSiO_4$ phases at 1200 and 1430°C practically do not differ one from another, whereas the $KAlSiO_4$ formed at 1300°C differs from both phases by having drastic changes in the magnitude of reflections (Fig. 4) within the 2Θ angle interval 20–30°. Comparison of XRD powder patterns of these phases (Table 4) shows that their crystal lattices are similar. Accordingly all three patterns are indexed on the same triclinic lattice (Table 1).

The qualitative differences between the $KAlSiO_4$ phase formed at 1300°C and both $KAlSiO_4$-O_1 and $KAlSiO_4$-O_2 phases are noticeable in their ^{29}Si and ^{27}Al solid-state MAS NMR spectra, as well as on infrared absorption spectra. All three aforementioned $KAlSiO_4$ phases have the ^{29}Si chemical shifts at −89 and −98 ppm which points to the same Si(4Al) environment. However, from Fig. 5d, it can

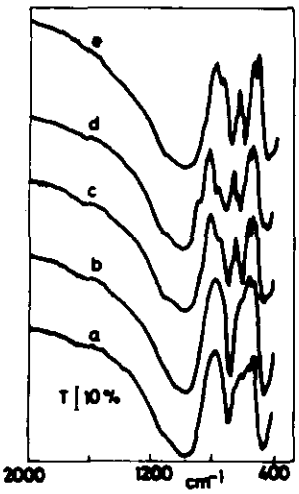

FIG. 6. Infrared absorption spectra of the investigated $KAlSiO_4$ polymorphs: (a) synthetic kaliophilite, (b) kalsilite, (c) $KAlSiO_4$-O_1 phase. (d) $KAlSiO_4$-ANA phase, and (e) $KAlSiO_4$-O_2 phase.

be seen that the $KAlSiO_4$ phase formed at 1300°C has a changed intensity ratio for chemical shifts at −89 and −98 ppm with respect to that of the $KAlSiO_4$-O_1 and $KAlSiO_4$-O_2 (Figs. 5c and 5e) phases. This points to a possible reorientation of SiO_4 tetrahedra in the structure of the $KAlSiO_4$ obtained at 1300°C relative to the $KAlSiO_4$-O_1 and $KAlSiO_4$-O_2 phases. On the basis of the shifts observed it may be concluded that in the structure of the $KAlSiO_4$ phase formed at 1300°C as well as in $KAlSiO_4$-O_1 and $KAlSiO_4$-O_2 phases, Si^{4+} cations are located at least in two nonequivalent symmetrical positions. The same positions of ^{29}Si chemical shifts in all three $KAlSiO_4$ phases (1200, 1300, and 1430°C) (Table 2), together with presented IR and XRD results, suggest the similar framework topologies in their crystal structures.

An additional support for this statement is obtained from ^{27}Al MAS NMR spectra of $KAlSiO_4$ phases, Figs. 5c–5e and Table 2. All three spectra display the same chemical shfit at 65.7 ppm which indicates a tetrahedral coordination of Al^{3+} cations. From Figs. 5c–5e, it is apparent that each of the $KAlSiO_4$ phases displays in the ^{27}Al spectra a shoulder near 60 ppm. Although the peaks at 65.7 ppm are not resolved, the shoulders at 60 ppm point to the presence of at least one additional symmetry-nonequivalent position of tetrahedrally coordinated Al^{3+} cations in these structures, which is consistent with the measured ^{29}Si chemical shifts.

Our ^{29}Si and ^{27}Al MAS NMR spectra could be compared only with data presented for the $KAlSiO_4$-O_1 phases (35). But, it should be noted that both presented spectra for the $KAlSiO_4$-O_1 phases have a shift for Si(3Al) environment what indicates a disorder of T cations in the framework. Efforts to simulate the NMR spectrum using the correlation given by Ramdas and Klinowski (43) and the proposed structure (42) did not explain the Si(4Al) shift near −85 ppm on both $KAlSiO_4$-O_1 samples (35). Our experiments gave opposite results: ^{29}Si chemical shifts at −85 ppm was not observed but two intense at −89.1 and −98.0 ppm, were measured. We believe that both these shifts arise from Si(4Al) environment. The latter assumption is strongly supported by completely ordered frameworks of the starting K-LTA zeolite (29) and the obtained synthetic kaliophilite and kalsilite (at 1000 and 1100°C, respectively); see Figs. 5a and 5b and Table 2. In the course of the reconstructive transformation of kalsilite into the $KAlSiO_4$-O_1 phase, if the rules given by Loewenstein (44) and Dempsey *et al.* (45) are obeyed, then the $KAlSiO_4$-O_1 phase formed by the topotactic transformation from the ordered kalsilite framework also should be ordered. According to the presented MAS NMR resutls, this conclusion must be valid for both polymorphs formed at 1300 and 1430°C.

The IR absorption spectrum (Fig. 6d and Table 3) of the $KAlSiO_4$ phase at 1300°C is almost identical to those of the $KAlSiO_4$-O_1 and $KAlSiO_4$-O_2 polymorphs. Some minor differences between them appear in the absorption bands within the 600–800 cm^{-1} (ν T–O–T symmetrical stretching mode) and the 400–500 cm^{-1} (δ O–T–O bending mode) regions. These results as well as the above-mentioned ^{29}Si and ^{27}Al MAS NMR spectra suggest a structural similarity for $KAlSiO_4$ phases synthesized in the temperature range 1200–1430°C.

All attempts to identify a $KAlSiO_4$ phase at 1300°C in the JCPDS file were unsuccessful, but it is very similar to that of synthetic leucite (JCPDS card 38-1423). Most of the reflections from the XRD powder pattern of $KAlSiO_4$ phase synthesized at 1300°C (Table 4) could be indexed on the tetragonal cell (4) in space group $I4_1/a$, but this could not be done with numerous superstructure lines. Numerous efforts to index the whole pattern of this phase on a doubled leucite cell or a multiplied $KAlSiO_4$-O_1 cell (7, 8) were not successful. However, the indexing based on a distorted leucite unit cell in triclinic symmetry (Tables 1 and 4) was successful. Here we want to emphasize that the leucite-like $KAlSiO_4$ phase formed at 1300°C has been observed by several authors (7, 17, 20) and interpreted as the leucite $KAlSiO_2O_6$. A thorough interpretation of irreversible formation of leucite as a result of volatilization of K from the crystals of kalsilite, $KAlSiO_4$-O_1, and kaliophilite may be questioned. In our opinion in all cases the phase with the $KAlSiO_4$ composition was considered. A preliminary study of the crystal structure of the $KAlSiO_4$ polymorph (at 1300°C) by the Rietveld method (34) in the nonadequate $I4_1/a$ space group (4) indicates the same topology of (Si, Al)O_4 framework as in leucite. The arguments in favor of the ordering of T(Si, Al) cations in the ANA framework have been presented

in our previous paper (22) and in the discussion on MAS NMR results. In accordance with the aforesaid discussion, the $KAlSiO_4$-ANA phase formed at 1300°C is a new phase and a polymorph in the KALSI system (Fig. 1b); it is located on the $KAlO_2$–SiO_2 (7) interface and situated between the low $KAlSiO_4$-O_1 and high $KAlSiO_4$-O_2 phases. According to the Loewenstein rule (44) $KAlSiO_4$-ANA phase is a secondly synthesized ANA-type end member (22) of the zeolite framework having the ratio Si/Al = 1.

According to presented results the polymorphous transitions synthetic kaliophilite → kalsilite and low $KAlSiO_4$-O_1 → $KAlSiO_4$-ANA → high $KAlSiO_4$-O_2 are displacive, while the transformation between the kalsilite → low $KAlSiO_4$-O_1 has a reconstructive character.

Here we want to emphasize the structural reversibility of the polymorphic transitions $KAlSiO_4$-O_1 → $KAlSiO_4$-ANA → $KAlSiO_4$-O_2. This type of reversible structural transition where low and high polymorphs are structurally equivalent, is characteristic of other catonic forms of the LTA precursor. For example, the high-temperature transformation of Na-LTA (25) has the following scheme: low carnegieite → nepheline → high carnegieite. In the case of the Rb-LTA precursor, the high temperature polymorphic transformation (34) can be represented as follows: low $RbAlSiO_4$-ANA → $RbAlSiO_4$-ABW → high $RbAlSiO_4$-ANA.

The reversibility of the structural transformations between the ABW- and ANA-type frameworks, observed at Cs-LTA (22) (ABW → ANA) and Rb-LTA (ANA → ABW → ANA) precursor, suggests similarities from a topological point of view. Our results obtained on K-LTA precursor ($KAlSiO_4$-O_1 → $KAlSiO_4$-ANA → $KAlSiO_4$-O_2 transitions) support a possible topological identity of ABW and ANA types of aluminosilicate frameworks. The final proof of the aforementioned presumption will be obtained from crystal structure measurements.

CONCLUSION

The significance of LTA zeolite frameworks as precursors for the synthesis of new aluminosilicates is shown in the present paper and in previous papers (21, 22).

The present study describes conditions for polymorphous transformations in the system K_2O–Al_2O_3–SiO_2, on the $KAlO_2$–SiO_2 interface. In the process of thermally induced phase transformation of K-LTA zeolite precursor, two new $KAlSiO_4$ polymorphs were synthesized. The synthetic kaliophilite is characterized by an ordered tridymite framework topology as is kalsilite. The second new phase, named $KAlSiO_4$-ANA, has an ordered framework topology very similar to the leucite. This study confirmed the existence of $MAlSiO_4$ (M = K, Cs) phases on the $MAlO_2$–SiO_2 interface, having an ordered ANA-type framework topology.

ACKNOWLEDGMENTS

We thank Mr. Dj. Cvijovic for MAS NMR analyses, Dr. U. Mioc for infrared spectra and Dr. M. Tomasevic-Canovic for thermal analyses. We thank the referees for useful constructive criticism of the paper. The authors are grateful to the Serbian Republic Research Fund for financial support.

REFERENCES

1. J. F. Schairer and N. L. Bowen, *Am. J. Sci.* **253,** 681 (1955).
2. J. V. Smith, "Feldspar Minerals, Crystal Structure and Physical Propeties." Springer-Verlag, Berlin, 1974.
4. D. R. Peacor, *Z. Kristallogr.* **127,** 213 (1968).
4. F. Mazi, E. Galli, and G. Gottardi, *Am. Mineral.* **61,** 108 (1976).
5. T. Grogel, H. Boysen, and F. Frey, *Acta Crystallogr. Sect. A* **40S,** C256 (1984).
6. W. M. Meier and D. H. Olson, "Atlas of Zeolite Structure Types." Structure Commission of the International Zeolite Association, Juris, Zurich, 1978.
7. L. P. Cook, R. S. Roth, H. S. Parker, and T. Negas, *Am. Mineral.* **62,** 1180 (1977).
8. J. V. Smith and O. F. Tuttle, *Am. J. Sci.* **255,** 282 (1957).
9. G. Kunze, *Heidelb. Beitr. Mineral. Petrog.* **4,** 99 (1954).
10. M. J. Buerger, *Am. Mineral.* **39,** 600 (1954).
11. R. N. Abbott, *Am. Mineral.* **69,** 449 (1984).
12. A. J. Perota and J. V. Smith, *Mineral. Mag.* **35,** 588 (1965).
13. W. A. Dollase and W. P. Freeborn, *Am. Mineral.* **62,** 336 (1977).
14. Y. Andou and A. Kawahara, *Mineral. J.* **12**(4), 153 (1984).
15. Y. Andou and A. Kawahara, *Mineral. J.* **11**(2), 72 (1982).
16. R. A. Lange, I. S. E. Carmichael, and J. F. Stebbins, *Am. Mineral.* **71,** 937 (1986).
17. C. Capobianco and M. Carpenter, *Am. Mineral.* **74,** 797 (1989).
18. A. Kawahara, Y. Andou, F. Marumo, and M. Okuno, *Mineralogical J.* **13**(5), 260 (1987).
19. G. R. Rigby and H. M. Richardson, *Mineral. Mag.* **28,** 75 (1947).
20. D. Cellai, M. Carpenter, and P. Heaney, *Eur. J. Mineral.* **4,** 1209 (1992).
21. V. Dondur and R. Dimitrijevic, *J. Solid State Chem.* **63,** 46 (1986).
22. R. Dimitrijevic, V. Dondur, and N. Petranovic, *J. Solid State Chem.* **95,** 335 (1991).
23. J. M. Newsam, *J. Phys. Chem.* **92,** 445 (1988).
24. P. Norby, *Zeolites* **10,** 193 (1990).
25. M. Ristic, N. Petranovic, M. Susic, V. Petrovic, and R. Dimitrijevic, "Science of Ceramics," (H. Hausner, Ed.), Vol. 10, p. 359. Deutsche Keramische Gesellschaft, Cologne" 1980.
26. N. Petranovic and R. Dimitrijevic, *Thermochim. Acta* **84,** 227 (1985).
27. V. Dondur, A. Kremenovic, and R. Dimitrijevic, Zeolites, submitted for publication.
28. P. C. W. Leung, K. B. Kunz, K. Seff, and I. E. Maxwell, *J. Phys. Chem.* **79,** 2157 (1975).
29. J. J. Pluth and J. V. Smith, *J. Phys. Chem.* **83,** 741 (1979).
30. P. E. Werner, L. Eriksson, and M. Westdahl, *J. Appl. Crystallogr.* **18,** 367 (1985).
31. J. W. Visser, *J. Appl. Crystallogr.* **2,** 89 (1969).
32. R. G. Garvey, *Powder Diffr.* **1,** 114 (1986).
33. W. Appel, J. Ihringer, K. Knorr, and W. Prandl, *Zeolites,* **7,** 423 (1987).
34. R. Dimitrijevic and V. Dondur, To appear.
35. J. F. Stebbins, J. B. Murdoch, I. S. Carmichael, and A. Pines, *Phys. Chem. Miner.* **13,** 371 (1986).

36. G. Hovis, D. Spearing, J. Stebbins, J. Roux, and A. Claire, *Am. Mineral.* **77,** 19 (1992).
37. C. M. B. Henderson and D. Taylor, *Mineral Mag.* **52,** 708 (1988).
38. J. V. Smith, *Chem. Rev.* **88,** 149 (1988).
39. J. V. Smith, *Am. Mineral.* **62,** 703 (1977).
40. O. F. Tuttle and J. V. Smith, *Am. J. Sci.* **256,** 571 (1958).
41. J. S. Lukesh and M. J. Berger, *Am. Mineral.* **27,** 226 (1942).
42. M. Gregorkiewitz and H. Schaffer, *in* Proceedings, Sixth European Crystallographic Meeting, Barcelona, Spain, 1980.
43. S. Ramdas and J. Klinowski, *Nature* **308,** 521, (1984).
44. W. Loewenstein, *Am. Mineral.* **39,** 92 (1954).
45. E. Dempsey, G. H. Kuhl, and D. H. Olsen, *J. Chem. Phys.* **73,** 387 (1969).